PCCP

Dynamics and spin relaxation of tempone in a host crystal. An ENDOR, high field EPR and electron spin echo study†

Antonio Barbon,[a] Marina Brustolon,*[a] Anna Lisa Maniero,[a] Maurizio Romanelli[b] and Louis-Claude Brunel[c]

[a] *Università di Padova, Dipartimento di Chimica Fisica, Via Loredan 2, 35131 Padova, Italy. E-mail: M.Brustolon@chfi.unipd.it; Fax: 39-049-8275135; Tel: 39-049-8275680*
[b] *Università di Firenze, Dipartimento di Chimica, Via G. Capponi 9, 50121, Firenze, Italy*
[c] *National High Magnetic Field Laboratory, 1800 East P.Dirac dr., Tallahassee, FL 32310, USA*

Received 28th April 1999, Accepted 15th July 1999

We studied in the temperature range 4–300 K the dynamics and the electron spin echo decay of the radical 4-oxo-2,2,6,6,-tetramethyl-1-piperidinyloxyl (tempone) doping substitutionally a single crystal of the diketone 2,2,4,4-tetramethyl-cyclobutan-1,3-dione. Electron nuclear double resonance (ENDOR) and high field electron paramagnetic resonance (EPR) spectra (110 GHz) displayed three types of motion: interconversion between twisted-crossover conformations, rotation of the methyl groups and libration of the radical in the crystal matrix. At room temperature all the motions are fast, and they reach the slow motion régime each at a different temperature, being all slow below 80 K. An approximate value of 9 kJ mol^{-1} for the energy barrier hindering the rotation of the tempone methyl groups is estimated. At low temperature their motion is too slow to give any contribution to the echo decay. The echo decays as a linear exponential in the range 100–300 K, due to the radical motions. At $T < 100$ K the interaction with the methyl protons of the matrix is the dominant dephasing mechanism, and the echo decays as a gaussian. At $T < 20$ K it depends on the square root of the time. Echo decays and electron spin echo envelope modulations (ESEEM) are simulated by using the available theoretical models. A damping of ESEEM superimposed to the echo decay is discussed.

Introduction

By means of the analysis of the electron spin echo decay of nitroxide radicals, rich information can been obtained on the dynamical and structural properties of condensed phases of different types (see for example ref. 1–4).

Several models have been developed to interpret the echo decay, in particular considering the spin relaxation due to dipole–dipole, fine and hyperfine interactions of the probe with the neighbouring radicals and nuclei of the matrix.[5,6] These models allow important information to be obtained from the decay function and from the echo envelope modulation (ESEEM), such as the mobility of the probe, its concentration, the type and number of nuclei surrounding it. So, electron spin echo (ESE) studies together with computer simulations of continuous wave (cw)-electron paramagnetic resonance (EPR) spectra allowing the inclusion of the effects of slow motions are in principle very important in getting information on the structure of complex supramolecular phases.

However, some ambiguity is present in the literature in evaluating the role of intramolecular motions in the probes themselves in dephasing the spin packets. In particular, the rotational motion of methyl groups in nitroxides at very low temperature is considered by some authors as an important cause of spin relaxation,[7] whereas other authors neglect it.[8] Moreover, the possible interconversion between different ring conformations is often ignored.

One of the more popular nitroxide radicals is tempone (4-oxo-2,2,6,6,-tetramethyl-1-piperidinyloxyl). This radical has been studied in many different systems by different EPR spectroscopies, such as continuous wave X-band EPR and W-band EPR (HF-EPR),[9] electron nuclear double resonance (ENDOR)[10–12] and electron spin echo (ESE) spectroscopy.[8,13,14]

We decided to study a model system doped with tempone by different cw-EPR techniques (X-band and high field EPR, ENDOR), and by ESE at different temperatures, trying to correlate the information obtained on the dynamics of the radical from the different experiments. The model system we chose is a single crystal of a diketone host (2,2,4,4-tetramethyl-cyclobutan-1,3-dione, TMCD), that is able to give substitutional mixed crystals with tempone. This system was studied in the past by X-band EPR and ENDOR,[10] and it promised to be sufficiently simple to allow a clear determination of the dynamical processes acting at the different temperatures.

We studied the dynamical properties of the radical in a large temperature range (4–300 K), exploring three different types of motions and their importance in determining the echo decay parameters.

Experimental

The crystals were prepared by slow sublimation of a weighted amount of TMCD and tempone 100 : 1 at room temperature under vacuum using a cold finger. TMCD crystallizes in the monoclinic system, space group $C2/m$ with $a = 6.55$, $b = 10.26$, $c = 6.43$ Å, $\beta = 104°$ and $Z = 2$.[15] The deuterated tempone was prepared by stirring an alkaline heavy water solution of the radical for 5–6 h at 40 °C.[10]

† Presented at the 32nd Annual International Meeting of the Royal Society of Chemistry's ESR Group, The University of York, 11th–15th April, 1999.

For ENDOR experiments a Bruker EN801 ENDOR cavity was used. The radiofrequency (RF) signals were generated from a Bruker ESP360 DICE ENDOR module followed by an ENI 3200L RF power amplifier. The sample temperature was controlled with a helium gas flow cooling system (Oxford ESP900 cryostat). The microwave power was between 5 and 20 mW. The radiofrequency was modulated with a frequency depth of 70 kHz, a modulation frequency of 12.5 kHz, an RF power of *ca.* 300 W, a scan time of 20 s; the receiver gain was 8×10^4, the signal to noise ratio was improved by accumulation of 20 to 120 scans.

Hahn echo experiments were run with a Bruker ESP380 instrument equipped with an overcoupled Bruker dielectric cavity. The cavity was inside a CFR934 Oxford cryostat cooled with helium vapours.

Pulses of 16 and 32 ns were used, at variable microwave power in order to test the dependence of the echo decays on the turning angles. Series of measurements with turning angles $\pi/2$ and π in the temperature range 4–300 K were performed. The minimum distance between pulses was 120 ns.

HF-EPR spectra were recorded at the high field electron magnetic resonance facility of the National High Magnetic Field Laboratory in Tallahassee, Florida. The EPR spectrometer is of similar design to the instrument described by Mueller *et al.*,[16] except for the following modifications: the sources are Gunn diodes oscillators (from Abmm, Paris), equipped with Schottky diode harmonic generators; the magnetic field is provided by a 15/17 T (at 4.2 and 2.2 K, respectively) superconducting Oxford Instruments magnet, and the detector is a 'hot electron' InSb bolometer (from QMC, London). The spectra are recorded in the magnetic field first derivative mode.

Theory

Electron spin echo decay

The relative importance of the different intrinsic relaxation processes producing ESE dephasing at a given temperature depends on the concentration of the radicals, on their residual mobility, and on the nuclear spins present in the diamagnetic matrix.

We can distinguish between the spin relaxation mechanisms intrinsic to the sample, and those due to the experiment itself, *i.e.* due to the perturbing effect of the microwave pulses (instantaneous diffusion, ID). It is customary to distinguish between the spin packets affected by the pulses (spin A) and those not affected (spin B). The instantaneous diffusion depends on the concentration of spin A, and on the extent of the perturbation created by the pulses on them, namely on the tilting angle of magnetisation of the single spin packets, which depends on the microwave power and on the pulse length. Instantaneous diffusion gives rise to exponential decay, with an exponent linear in time. The concentration of spin A depends in turn on the total radical concentration and on the spectral range affected by the pulses. If the radicals are distributed at random in the matrix, so that the inter-radicals average distance can be correlated with the total concentration, ID effects can be seen for a molar concentration $C >$ *ca.* 10^{-4} M.[5,17]

Among the intrinsic relaxation mechanisms we can envisage those due to the time fluctuation of the parameters of the spin hamiltonian, and those due to the time fluctuation of the coupled spins. These mechanisms are known, respectively, as first kind and second kind ones.[18]

The relaxation mechanisms of the first kind affect the T_2 of the single spin packets, and the echo decays as a linear exponential. The time dependence of the different terms of the spin hamiltonian can be due to intra- and intermolecular motions.

The spin hamiltonian for a nitroxide radical k in the present system, neglecting the quadrupolar interaction is given by

$$H_k = \nu_{ek} m_{sk} + \sum_i (-\nu_{ni}\boldsymbol{h} + m_{sk}\boldsymbol{h}\boldsymbol{T}_i)\boldsymbol{I}_{ni} + \sum_j \boldsymbol{S}_j \boldsymbol{D}_j \boldsymbol{S}_k \quad (1)$$

where $\boldsymbol{h}$ is the unit vector in the direction of the external field, ν_{ek} is the electron Larmor frequency, ν_{ni} is the nuclear frequency of the i-th nucleus, $\boldsymbol{T}_i$ are the hyperfine tensors for the interactions of the ^{14}N and the proton nuclei with the electron, $\boldsymbol{D}_j$ is the fine tensor for the interaction with other radicals, and the other symbols have the usual meaning. In general the intermolecular motions modulate all the tensors in eqn. (1), and the intramolecular ones modulate mainly the hyperfine tensors $\boldsymbol{T}_j$. The contribution to the relaxation due to the inter- and intramolecular motions of the probe are discussed in the next section.

We want to focus now on the relaxation mechanisms of the second type, due to a time dependent dipolar interaction of spin A with other flipping spins in the system. The latter ones can be the electron spin packets not affected by the pulses, and the nuclei of the matrix.[5,6] We briefly summarise the theory of echo decay due to these interactions. For a full treatment of the problem we refer to some papers given in the text.

Because of the time dependent intermolecular and intramolecular interactions of the probe modulating the parameters of the spin hamiltonian, and because of the fluctuation of the $\boldsymbol{I}$ spins and other radical electron m_{sj} spins (A or B spins), the precession of the k-th spin is dephased from the Larmor frequency by the time-dependent quantity $\delta\nu_{ek}(t)$. The echo intensity is proportional to the magnetisation M_y at time τ after a pulse sequence $(\pi/2)_x\tau(\pi)_x$. M_y can be calculated using the density matrix formalism.[19]

The echo signal $E(2\tau)$ (at time τ after the second pulse) of n identical A spins with ν_{ek} resonance frequency is given by

$$E(2\tau) \propto n(\nu_{ek})\mathrm{Re}[\exp(2\pi \int_0^{2\tau} s(t')\delta\nu_{ek}(t')\mathrm{d}t')] \quad (2)$$

where $s(t') = \pm 1$ ($+1$ for $0 < t' < \tau$, -1 for $\tau < t' < 2\tau$).

When the concentration of the spins is low, the principal mechanism of relaxation due to the other electron spins is given by the time fluctuations of their z component because of the spin–lattice relaxation T_1^{-1}. For the fluctuations of the z component of the electron spin two models have been assumed, the Gauss–Markov and the sudden jump one. Using the two models, and averaging on distributions of B spins and on the time, the decays reported in Table 1 are obtained.

All the relations in Table 1 are stretched exponential functions:

$$I(t) = A_1 \, \mathrm{e}^{-(t/\tau_1)^{x_1}} \quad (3)$$

where $I(t)$ is the intensity of the echo, t is the time corresponding to the maximum of the echo after the last pulse.

From the value of the exponent x_1 one can therefore obtain important information on the mechanism determining the relaxation.

Electron spin echo modulation

The nuclear modulation of the echo decay due to a single coupled proton is given by (ref. 20):

$$V_{\mathrm{mod}}(2\tau) = 1 - 2k \sin^2\left(\frac{\omega_+ \tau}{2}\right)\sin^2\left(\frac{\omega_- \tau}{2}\right) \quad (4)$$

where τ is the delay between pulses, $\nu_\pm = \omega_\pm/2\pi$ are the ENDOR frequencies, $k(\nu_H B/\nu_+ \nu_-)^2$ is the so called modulation depth (ν_H is the free proton frequency).

Both the $\nu_\pm$ and the parameter B can be calculated from the hyperfine tensors $\boldsymbol{T}_H$.[21] If the orientation of the magnetic field $\boldsymbol{h}$ in the molecular axes system is given by the direction

Table 1 Analytical expressions obtained from eqn. (2) for given models and approximations. $\Delta\omega_B$ is proportional to the dipolar magnetic field due to spin *B*s on spin *A*s, τ is the time between pulses and τ_c is T_1 for the electron spins. The parameter *m* is defined in the Results section

Relaxation mechanism	Expression for the decay	Type of motion	Ref.
B nuclear spin flip–flop	const/exp($-m\tau^{7/4}$)		6
B electrons spin flip	const/exp($-2\Delta\omega_B\sqrt{2\tau\tau_c/\pi}$)	Gauss–Markov model $\tau/\tau_c \gg 1$	19
B electrons spin flop	const/exp($-2\Delta\omega_B\sqrt{4\tau^3/(3\pi\tau_C)}$)	Gauss–Markov model $\tau/\tau_c \ll 1$	19
B electrons spin flip	const/exp($-2\Delta\omega_B\sqrt{\tau\tau_c/\pi}$)	Sudden jump model $\tau/\tau_c \gg 1$	19
B electrons spin flip	const/exp($-2\Delta\omega_B\tau^2/\tau_c$)	Sudden jump model $\tau/\tau_c \ll 1$	19

cosines (*l*, *m*, 0) for a proton we have:[22]

$$\nu_\pm = [(\nu_H \pm A_H/2)^2 + B^4/4]^{1/2}$$
$$A_H = l^2 T_{H_{xx}} + m^2 T_{H_{yy}} + 2lm T_{H_{xy}}$$
$$B^2 = (lT_{H_{xz}} + mT_{H_{yz}})^2 + [lm(T_{H_{xx}} - T_{H_{yy}}) - (l^2 - m^2)T_{H_{xy}}]^2 \quad (5)$$

Thus the echo is modulated at ν_+, ν_-, at their sum and difference. Its amplitude depends on the non-diagonal terms of the hyperfine tensor $\boldsymbol{T}_H$.

Results

X-band EPR

In the single crystals of tempone–TMCD the EPR spectrum of tempone is composed of three lines due to the coupling with the nitrogen ranging between *ca.* 6 and 30 G depending on the orientation of the crystal in the magnetic field.

In the previous paper[10] the $\boldsymbol{g}$ and $\boldsymbol{T}_N$ tensors were determined. Only one type of radical in a unique crystal site was detected. From the principal directions of the tensors as compared with the crystal structure of the host, it was found that tempone is oriented with the N–O bond collinear to the C=O bonds of the host. Moreover, the principal directions corresponding, respectively, to the maximum principal value of the nitrogen hyperfine tensor, and to the minimum principal value of the $\boldsymbol{g}$ tensor, were coincident within the experimental error, and this direction was also found parallel to the twofold *b* axis of the host crystal.[10] The previous principal direction had been attributed therefore to the axis of the π orbital of the N–O group bearing the unpaired electron. As explained later, in the present work we have found that the radical is librating rapidly in the host lattice, and the axis of the π orbital is jumping between two equivalent orientations symmetrically disposed with respect to the crystallographic *b* axis. Therefore, the axis found in ref. 10 is the average orientation of the *Z* axis of the π orbital, we will call this axis $\langle Z \rangle$, see Fig. 1. The results are reported in Table 2. As one can see, the $\boldsymbol{T}_N$ tensor is approximately axial, whereas the $\boldsymbol{g}$ tensor is not, the largest principal value corresponding to the principal direction along the N–O bond.

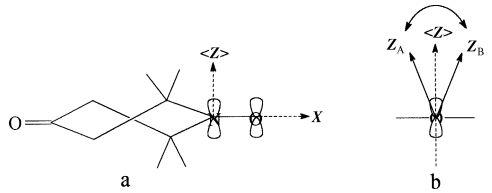

Fig. 1 Tempone in twisted-crossover conformation. a and b are, respectively, the side view and the view along the *X* axis, to put in evidence the libration around this axis.

At high microwave power weak sidebands due to forbidden transitions involving a weakly coupled proton can be seen at a distance from the main lines equal to the free proton frequency. The EPR linewidths vary with the temperature. In a single crystal oriented in the magnetic field so to have the maximum ^{14}N splitting, the linewidth of the central line is 0.30 mT at room temperature and 0.32 mT at 130 K. At 50 K a further unresolved hyperfine structure appears that broadens the line to 1.15 mT. At 10 K the lines overlap and all the structure is almost lost.

The X-band EPR spectra are anyway too poor in resolution to extract more information, and the process responsible for the temperature dependent linewidths can be studied easily by the HF-EPR spectra, as reported below.

ENDOR

Single crystal and powder ENDOR spectra were measured in the range 4–300 K. A complete determination of hyperfine tensors of the methyl protons by ENDOR in a single crystal of TMCD doped with tempone deuterated in the methylene positions has been done in ref. 10 at $T = 190$ K. The conclusions were that at 190 K the methyl groups are rotating fast, whereas the interconversion between the two possible twisted-crossover conformations is slow. The ENDOR study has been completed in the present work by analysing the proton ENDOR spectra in a wider temperature range. The crystal has been oriented with the magnetic field along the $\langle Z \rangle$ axis, which is parallel to the binary axis of the crystal. We expect therefore for this orientation a particularly simple ENDOR spectrum, since all the protons related by the π rotation around the binary symmetry axis will be magnetically equivalent.

The intensity of the ENDOR transitions depends strongly on the temperature: starting from room temperature, the ENDOR signals increase in intensity down to 190 K, then the intensity decreases. At 100 K no ENDOR signal is detectable. By further cooling of the system, the ENDOR signals reappear, passing though a maximum at around 50 K.

The pattern of the spectrum is also influenced strongly by temperature. At 300 K (see Fig. 2a) the proton ENDOR spectrum centered at ν_H shows quite broad lines: the two pairs of lines with the largest hyperfine splitting correspond to frequency distances of 2.1 and 3.1 MHz, and a strong wide band

Table 2 $\boldsymbol{T}_N$ and $\boldsymbol{g}$ tensors principal values for tempone in TMCD as obtained in ref. 10. The axes *X* and $\langle Z \rangle$ correspond, respectively, to the direction of the N–O bond and to the average orientation of the axis of the π orbital

$\boldsymbol{T}_N$/MHz	$\boldsymbol{g}$
$T_{\langle Z \rangle} = 91.06$	$g_{\langle Z \rangle} = 2.0026$
$T_\perp = 15.49$	$g_X = 2.0094$
$T_\perp = 16.27$	$g_Y = 2.0066$

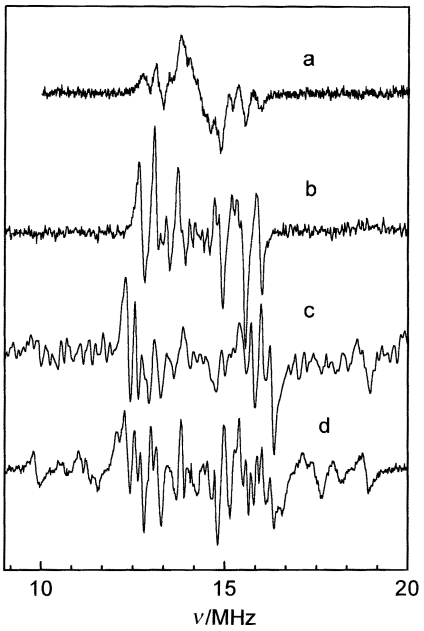

Fig. 2 ENDOR spectra of tempone in a TMCD single crystal with the crystallographic axis $b//B_0$ (a: $T = 300$ K; b: $T = 190$ K; c: $T = 80$ K; d: $T = 50$ K). The spectra are obtained by pumping the ESR transition corresponding to $M_I = -1$ for ^{14}N. The spectra have been recorded with a radiofrequency modulation depth of 70 kHz, a radiofrequency power of 300 W, and a microwave power of 15 mW. The spectra are averages of several sweeps, from the top to the bottom 20, 30, 60 and 70 sweeps.

due to the superposition of many lines corresponding to small hyperfine couplings is present at ν_H. At 230 K the lines are narrower. This is an indication that a relaxing mechanism for the proton transitions effective at higher temperature becomes less effective at lower temperature, due to the slowing down of the dynamical process responsible for the relaxation. A larger number of peaks can be resolved, whereas the width of the spectrum is nearly unmodified. At 190 K (Fig. 2b) the spectrum has still narrower lines. It shows a complex pattern with many peaks and resolved splittings ranging from 0.1 to 3.2 MHz. This spectrum, as reported above, has already been interpreted.[10] On a further lowering of the temperature the structure of the peaks at frequencies near ν_H is lost because the lines broaden, in particular the pairs with small hyperfine couplings. At 100 K no ENDOR signal is detectable, and the spectra can be recorded again at 80 K and below (see Fig. 2c). In the latter spectrum some lines are still broad as can be seen by comparing the spectrum with that at 50 K (Fig. 2d). The comparison of this latter spectrum with that at 190 K shows important changes. A larger number of ENDOR lines is found, covering a larger spectral range. At least six pairs of lines appear outside the range of the spectrum at 190 K, and it is possible to identify lines due to hyperfine splittings as large as 9.0 and 7.4 MHz.

The temperature dependence of the powder ENDOR spectra is the same as that found for the single crystal.

High-field EPR

The W-band EPR spectra have been recorded at different temperatures for two orientations of the crystals: $B_0//b$, and B_0 laying on a cone forming an angle of 30° with b. We remind that b is also a principal axis for both the average $\boldsymbol{T}_N$ and $\boldsymbol{g}$ tensors as determined at 190 K. The spectra corresponding to $B_0//b$ are given by three lines of the same width with a hyperfine splitting $A_N = 3.26$ mT from room temperature to 40 K. The linewidth increases on lowering the temperature, being 0.26 mT at room temperature and 0.6 mT at $T = 60$ K. Some spectra are reported in Fig. 3.

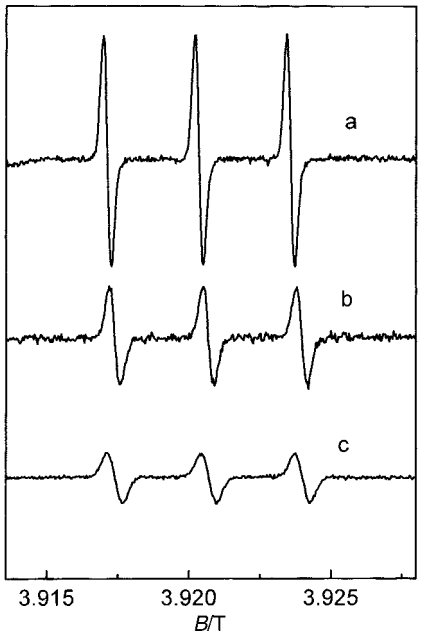

Fig. 3 W-band spectra of tempone in TMCD with the crystallographic axis $b//B_0$ (a: $T = 275$ K; b: $T = 140$ K; c: $T = 100$ K). $\nu = 109.945$ GHz, modulation amplitude = 0.01 mT.

The other series of spectra taken for $B_0 \wedge b = 30°$ are shown in Fig. 4. They depend strongly on the temperature. In the range from room temperature to 200 K the spectrum is still given by three lines, with a splitting of 2.89 mT, and temperature dependent linewidths. At $T > 250$ K the linewidths of the three lines are about the same, 0.4 mT. Weak lines that can be attributed to forbidden transitions can be seen between the main lines, see Fig. 4a. For $T < 250$ K the spectrum becomes clearly asymmetric, indicating a dynamical exchange process affecting both the hyperfine splitting and the g factor. At $T = 180$ K the linewidths are very large, see Fig. 4c; then at lower temperatures the spectrum is given by six lines, due to two 1 : 1 : 1 triplets with different g factors and hyperfine splittings, see Fig. 4e. The hyperfine splittings of the two trip-

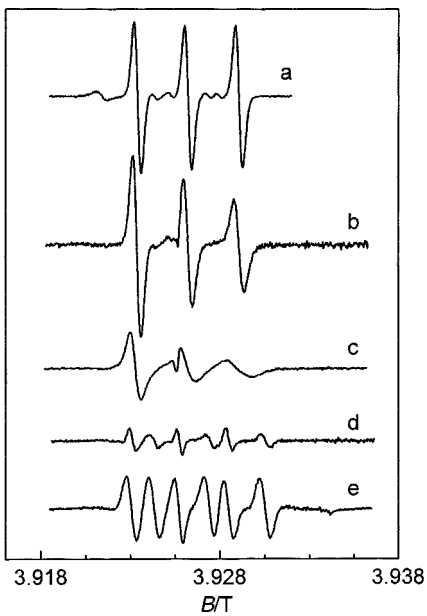

Fig. 4 W-band spectra of tempone in TMCD single crystal with the axis b forming an angle of 30° with B_0 ($\nu = 110.198$ GHz. a: $T = 276$ K, b: $T = 200$ K; c: $T = 180$ K; d: $T = 140$ K; e: $T = 110$ K). The spectra at different temperatures show the slowing down of the librational motion of the radical.

lets centered at high and low field are, respectively, 3.12 and 2.72 mT. The ΔB between the centers of the two triplets corresponds to $\Delta g = 9 \times 10^{-4}$.

ESE

At every temperature at which echoes can be observed, there is an echo modulation superimposed to the echo decay.

We fitted the experimental spectra by means of eqn. (4) combined with the stretched exponential decay of eqn. (3). A damping of the modulation depth (see discussion) has been introduced phenomenologically:

$$I_{tot}(t) = A_1 \, e^{-(t/\tau_1)^{x_1}} \prod_i \times \left[1 - 2k_i \, e^{-t/\tau_{dec}} \sin^2\left(\frac{\omega_{i+} t}{2}\right)\sin^2\left(\frac{\omega_{i-} t}{2}\right)\right] \quad (6)$$

Echo decays and echo modulations are treated in separate sections.

Echo decay

We verified that the contribution to the echo decay from instantaneous diffusion processes is not important, on the basis of the results of experiments run with increasing microwave power.[17] The dephasing due to instantaneous diffusion, in fact, depends on the tilting angle of the magnetization, and in the present case almost no dependence of the echo decays on the microwave power was found.

One can observe that for different temperature ranges, different decay laws are followed (see Table 3 and Fig. 5). At the highest temperatures the decay is linearly exponential, which is typical of relaxation processes dominated by T_2. In the range 130–210 K the echo is not detectable, the phase memory time being shorter than the dead time of the spectrometer (~80 ns). When the echo reappears below ~130 K, the decay follows a gaussian law. It is possible to note that τ_1 passes through a maximum at 80 K. Below 50 K it is mildly dependent on the temperature.

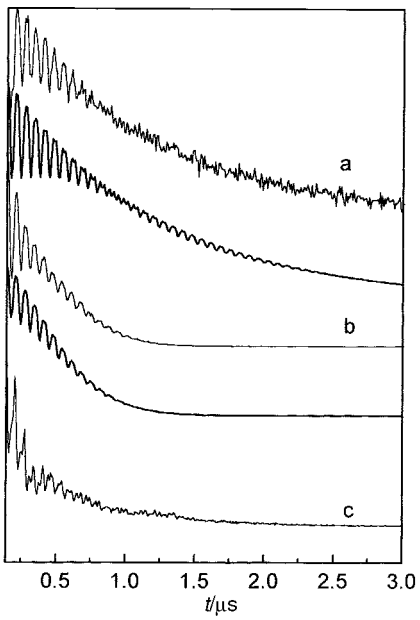

Fig. 5 Echo decays obtained with the crystallographic axis $b//B_0$(a: $T = 300$ K; b: $T = 50$ K; c: $T = 12$ K). The parameters of the echo experiment are reported in the text. For $T = 300$ K and $T = 50$ K: upper traces experimental, lower traces simulated. For $T = 12$ K only the experimental decay is reported. The decay at $T = 300$ K (curve a) is obtained from a crystal deuterated in the methylene positions. The simulation of the modulation is obtained by assuming a dipolar coupling with the twelve equivalent protons of the methyl groups of tempone, see text. The decay is fitted with a linear exponential. The simulation of the modulation at $T = 50$ K (curve b) is obtained by assuming a dipolar coupling with the twenty four equivalent protons of the methyl groups of the first shell of host molecules. The decay is fitted with a gaussian.

Table 3 Parameters of the stretched exponential eqn. (3) used to fit simple experimental echo decays

T/K	x_1	τ_1/μs
5	0.5	0.58
12	0.5	0.68
25	2	0.69
35	2	0.56
50	2	0.65
80	2	1.44
100	2	0.8
210	~1	0.22
260	~1	0.42
300	~1[a]	1.1[a]

[a] Tempone deuterated in the methylene positions.

A gaussian or pseudogaussian ($x_1 \sim 2$) decay of the echo is followed by samples for which fast flips of neighbour electron spins cause consistent spectral diffusion, or for samples for which relaxation is due to nuclear flip–flop. We considered that the latter relaxation mechanism is the important one at low temperature in our system, since the radical concentration is small enough to neglect the radical–radical interactions, and simulated the decays in the range 50–25 K for a relaxation due to nuclear flip–flop of the host matrix protons (see Table 1, first row). The parameter m has been obtained on the basis of the expression (ref. 6):

$$m \cong 2\pi\gamma_N^2 \hbar C_N^2 (3\gamma_N \gamma_e \hbar r_{N-N})^{3/4}/10 \quad (7)$$

A correct fit has been obtained by assuming an effective proton concentration C_N of 0.14 mol cm^{-3} (close to the experimental value of 0.18 mol cm^{-3}), and an average nucleus–nucleus distance r_{N-N} of 1.8 Å (proton–proton methyl distance).

It should be noted that, for very low temperatures (below 20 K), the echo decays follow an exponential law with square root time dependent exponent $x = 0.5$, see Table 3.

ESEEM: electron spin echo envelope modulation

We tried to simulate the ESEEM modulation at room temperature, as obtained on a TMCD crystal oriented with the b axis parallel to the magnetic field, and doped with tempone deuterated at the methylene positions. A particularly simple hyperfine coupling scheme is expected for this orientation, *i.e.* a coupling with the twelve methyl equivalent protons, by assuming a fast interconversion between two twisted crossover (t-c) conformations that allow the methyl groups to jump between the axial and equatorial positions. By averaging the methyl protons' tensors as obtained by ENDOR at 190 K,[10] we obtained a hyperfine tensor from which we deduced the ENDOR frequencies ν_+ and ν_- and the modulation depth k, see eqn. (5). We succeeded in simulating the ESEEM with twelve equivalent protons, with $\nu_+ = 14.83$ and $\nu_- = 14.29$ MHz ($\nu_H = 14.50$ MHz), see Fig. 5a. No modulation due to the methylene deuterons was observed.

On the basis of the evidences obtained on the temperature dependence of the motions of the radical, as discussed below, we expect a more and more complicated nuclear modulation scheme on decreasing the temperature. In particular, we expect that, due to the freezing of the intermolecular motion of the radical, matrix protons contribute to the modulation of the echo. We tried to simulate the echo modulation in the range 35–130 K assuming that the modulation was due to the first shell of matrix methyls. They are characterized by small

Table 4 Damping parameters τ_{dec} for modulation. This accounts for the lowering of the modulation depth with time

T/K	τ_{dec}/μs
5	0.6
12	0.7
25	0.8
260	1.2
300	1.1[a]

[a] Tempone deuterated in the methylene positions.

differences in the dipolar couplings, with ENDOR frequencies around ν_H. We fitted the experimental spectra by using 24 protons coupled to the radical with ENDOR frequencies $\nu_+ = 14.75$ and $\nu_- = 14.36$ MHz. The spectral resolution is of the order of $\Delta\nu = 1/2\pi T_2$, and for $T_2 \sim 0.4$ μs, $\Delta\nu \sim 0.3$ MHz, that means that we are not able to take into account the small differences within this range. The echo decay and simulation at $T = 50$ K are reported in Fig. 5b.

At still lower temperatures, an increasing number of frequencies in the modulation pattern can be noted, as expected due to the slowing down of all the motions, leaving a number of weakly coupled nonequivalent protons belonging probably both to the radical and to the matrix. In Fig. 5c the experimental echo decay for $T = 12$ K is reported.

To simulate correctly the echo modulations, a phenomenological dependence on the time (damping) of the modulation had to be introduced in eqn. (4). It has been done introducing a decay of the modulation depth $k(t)$ of the form $k\,e^{-t/\tau_{dec}}$ [see eqn. (6)]. The fitting values are collected in Table 4.

Discussion

Types of motions and effects on the cw-spectra

The dramatic temperature dependences of the cw EPR and ENDOR spectra indicate the presence of several motions of the radical in the matrix.

To make clear the grounds of our hypothesis on the nature of the motions, we outline in the following what are the effects one can guess on the different spectra due to different kinds of motions.

Interconversion between twisted-crossover conformations. Tempone is known to be in a twisted-crossover conformation (t-c), see Fig. 1.[10] It is also known that the radical in liquid solution at room temperature is rapidly interconverting between the two equivalent t-cs. The effect of a 'fast' interconversion in the crystal should be that the equatorial and axial methyl groups and methylene protons of the tempone radical become equivalent. If the interconversion is slow we expect to see in general the hyperfine coupling with two groups respectively of equatorial and axial methyl and methylene protons, apart from when the magnetic field is parallel or perpendicular to the C_2 axis of the twisted-crossover ring. We can compare these predictions with the ENDOR results. From the previous work on tempone–TMCD, at 190 K we determined by ENDOR the hyperfine tensors of the axial and equatorial methyl groups. Therefore, at 190 K the interconversion between the two t-c conformations is slow. As reported in the previous section, in the present investigation we found that the number of ENDOR lines for $T > 230$ K is reduced. The difference of the ENDOR spectra at $T = 190$ and 300 K can be seen in Fig. 2, where the averaging of the spectrum at higher temperature is very evident. Therefore we conclude that in the temperature range $300 > T/K > 230$ the interconversion between the two t-c conformations is fast.

Intermolecular librational motion. In the temperature range 160–200 K the W-band spectra reported in Fig. 4 depend strongly on the temperature, whereas the corresponding X-band ones are temperature independent in the same range.

Therefore we must assume that the radical is performing an intermolecular librational motion in the host matrix, jumping between two positions A and B, corresponding to different g factors. In the high field EPR spectra the Δg due to such a motion changes the central field of the EPR spectrum considerably more than at low field; we have ΔB(W-band) $\cong 10 \times \Delta B$(X-band). Therefore the timescale of the intermolecular motion is different for different resonance frequencies, and motions "fast" at X-band can become "slow" at W-band.

Let us assume that the motion is a libration around one of the principal axes of the magnetic tensors. The two positions A and B are then equivalent when the magnetic field B_0 is along a principal axis, and no effect due to the jump is expected in the spectra at any frequency, see Fig. 3. On the other hand, when B_0 is in a whatever orientation with respect to the radical, A and B are not equivalent anymore, see Fig. 4. In Fig. 4e we see the two spectra corresponding to the A and B sites in the slow motion régime. The two spectra show different g factors and also different ^{14}N hyperfine splitting. If the librational motion was around the Z axis we would expect that the ^{14}N hyperfine splittings for A and B sites would be very similar due to the near axiality of the $\boldsymbol{T}_N$ tensor in the XY plane, see Table 2.

Therefore we assume as the most probable hypothesis that the radical is librating around the X axis, see Fig. 1.

As a consequence the $\boldsymbol{T}_N$ and $\boldsymbol{g}$ tensors determined by the X-band EPR and ENDOR measurements in ref. 10 are average tensors, and in particular the principal direction corresponding to the maximum hyperfine splitting is the average position of the Z axis, $\langle Z \rangle$. However, since the tilting averaging angle is small, we can use their principal values to evaluate approximately the amplitude of the librational motion. From the values of the A_N splittings in spectra at low temperature, see Fig. 4e ($A_{N1} = 3.12$ mT and $A_{N2} = 2.72$ mT), we evaluate an angle of nearly 20° between the orientations of the Z axis reached during the exchange. The difference between the g factors obtained by taking the difference between the centers of the two triplets ($\Delta g = 9 \times 10^{-4}$), is compatible with this angle.

Methyl groups rotation. The ENDOR results at 190 K show that the methyl groups of tempone are rotating rapidly in the ENDOR timescale, since we determine a common tensor for all protons of each methyl group.

On the other hand, the proton ENDOR results at $T < 80$ K, see spectrum in Fig. 2d, show the presence of more lines, some at frequencies corresponding to larger hyperfine couplings, with respect to the 190 K spectrum (Fig. 2b). This effect must be attributed to a slowing down of a motion involving the relative positions of the radical protons with respect to the N–O group.

Therefore we conclude that at $T < 80$ K the methyl groups' rotation becomes slow on the ENDOR timescale. Each proton is in a fixed position with respect to the electron spin distribution, determined by the minima of the potential hindering the methyl rotation, and its hyperfine tensor is not averaged anymore by the motion. The actual positions of the potential minima are not known for tempone in TMCD. However, from the crystal structure of pure tempone[23] we obtained the positions of the methyl protons with respect to the molecular axes of the radical for that system.

By means of a McConnell–Strathdee calculation[24] by assuming $\rho_N = \rho_O = 0.5$ for the spin density distribution on the NO group,[10] we obtained six different pairs of symmetry

related tensors. Their positive principal values span an interval between 2.9 and 7.2 MHz, the largest principal values being 7.2, 7.1, 6.5 and 6.6 MHz.

The largest measured proton couplings at $T = 50$ K, see Fig. 2d, are 9.1, 7.6, 6.6 and 6.2 MHz. Taking into account that the minimum energy positions of the methyl protons in the TMCD crystal can be different with respect to those in the tempone crystal itself, the agreement supports our interpretation of the ENDOR spectrum at low temperature.

Relaxation mechanisms and electron spin echo decay

As discussed above, the temperature dependence of the EPR and ENDOR spectra of tempone in TMCD can be explained by assuming three different motions: (i) interconversion between twisted-crossover conformations, (ii) libration of the whole radical in the matrix, and (iii) rotation of methyl groups. The motions exchange the spectral lines of the interconverting species, and their effect depends on the rate of the interconversion and on the line separations in the low motion régime.

We can have some hints on the rates of the motions from the temperature range corresponding to the transition between the slow and fast motion régimes. It is well known to occur at temperatures at which the exchange rate becomes equal to the frequency separation of the exchanging lines.[25]

(i) From ENDOR spectra we know that the interconversion between t-c conformations becomes slow in the ENDOR timescale at $T < 230$ K. This means that, at $T \cong 230$ K, $\tau_I^{-1} \cong 2\pi\Delta A_H$, where τ_I^{-1} is the interconversion rate and ΔA_H is the variation of the hyperfine splittings of methyl and methylene protons during the conformational interconversion. From the hyperfine tensors $\boldsymbol{T}_{Hi}$ obtained by ENDOR we can estimate $2\pi\Delta A_H \cong 10^7$ s^{-1}. Therefore the conformational interconversion rate has the value $\tau_I^{-1} = 10^7$ s^{-1} at $T = 230$ K, and for this temperature we expect the maximum contribution of the latter motion to T_2^{-1} of the spin packets involved in the exchange.[25]

(ii) The spin relaxation effects due to the libration of the radical depend on the orientation of the crystal in the magnetic field. Each line at high temperature will split into two lines at low temperature, with resonance fields separation ΔB. If the libration rate is $\tau_R^{-1} > g\mu_B \Delta B/\hbar$, the fast exchange spectrum will be an averaged three line spectrum, if $\tau_R^{-1} < g\mu_B \Delta B/\hbar$ the slow exchange spectrum will be the superpositions of the two triplets corresponding to the two positions of the radical in the matrix. The maximum linewidth effect is expected for $\tau_R^{-1} \cong g\mu_B \Delta B/\hbar$. In Fig. 4e we can measure the field separation ΔB between each pair of split lines, which is ≈ 2 mT. In the same series, the spectrum with the largest linewidths is recorded at $T = 180$ K (Fig. 4c). Therefore we estimate $\tau_R^{-1} = g\mu_B \Delta B/\hbar$ with $\Delta B = 2$ mT at $T \approx 180$ K, corresponding to a libration rate of $\tau_R^{-1} = 3 \times 10^8$ s^{-1}. For X-band spectra the field separation between two exchanging lines at the same orientation would be about 0.2 mT, and therefore the libration motion is still fast at X-band at this temperature. The contribution to T_2^{-1} at X-band due to this motion can therefore be evaluated from the expression $T_2^{-1} = \tau_R\ (g\mu_B \Delta B/\hbar)^2$,[25] which corresponds to a value of $T_2^{-1} = 4 \times 10^6$ s^{-1}.

Therefore, the two motions described above will contribute in general to a fast relaxation in a temperature range with an upper limit $T \leqslant 230$ K.

As one can see in Table 3, the electron spin echo phase memory time (T_M) has a short value $T_M = 220$ ns at $T = 210$ K, and it becomes so short in the range 210 K $> T >$ 150 K that the echo is not detected any more since it decays during the deadtime. Moreover, the x_1 exponent in the range of temperatures 210–300 K is $x_1 = 1$, which is typical of spin relaxations determined by the T_2 values of the individual spin packets.[19] We can therefore conclude that in the range 150–300 K the phase memory time of the tempone radical is determined by relaxation mechanisms of the first kind, *i.e.* due to time fluctuations of the parameters of the spin hamiltonian.

(iii) The dephasing of ESE in nitroxide spin probes at low temperature has been attributed in some cases to the effect of the rotating methyl groups belonging to the radical itself. In the following we discuss this point.

From the ENDOR spectra we know that the tempone methyl groups rotation becomes slow in the ENDOR timescale at $T < 80$ K. Therefore we have for $T \approx 80$–90 K, $\tau_c^{-1} \approx 2\pi\Delta A_H$, where ΔA_H is the difference between the hyperfine interactions of the methyl proton for two positions exchanged during the rotation of the methyl group.

By taking for ΔA_H the minimum value of 1 MHz, we obtain for the latter temperature $\tau_c^{-1} \approx 6 \times 10^6$ s^{-1}.

The temperature variation of τ_c^{-1} follows the Arrhenius law:

$$\tau_C^{-1} = \tau_{\infty C}^{-1} \exp(-\Delta E/kT) \tag{8}$$

and therefore 6×10^6 s$^{-1} = \tau_{\infty c}^{-1} \exp(-\Delta E/k90)$. By assuming a value for $\tau_{\infty C}^{-1} = 10^{12}$ s^{-1},[26] we obtain $\Delta E/k \approx 1100$ K.

This value for the energy barrier hindering the rotational motion of the methyl groups can be compared with other values in the literature. The $\Delta E/k$ values hindering the motion of a methyl group linked to an aromatic carbon atom, or to an aliphatic one of the type CH_3CH_2R, span a range from 32 to 1000 K.[26] Unfortunately very few data can be found on the dynamics of methyl groups in molecules of the type $(CH_3)_2CR_2$, where two methyl groups are linked to the same carbon atom. In a previous work some of us have determined the energy barrier hindering the rotational motions of methyl groups belonging to *t*-butyl groups in the radical 4-methyl-2, 6-di-*t*-butylphenoxyl.[27] The energy barrier found for the less hindered methyl groups belonging to the *t*-butyl groups is $\Delta E/k = 1260$ K. Therefore the approximate value we have obtained for the methyl groups in tempone is a reasonable one.

Let us start to consider the effect of the methyl groups rotational motions for temperatures $T > 80$ K, where we are in the fast motion régime. The rotation produces time modulation of both the contact coupling and dipole coupling of the methyl protons with the unpaired electron. Therefore in the spin hamiltonian (1) there are time dependent spin operators producing secular ($\Delta m_s = 0$, $\Delta m_H = 0$), non-secular ($\Delta m_s = \pm 1$, $\Delta m_H = 0$) and pseudosecular ($\Delta m_s = 0$, $\Delta m_H = \pm 1$) relaxations.

For the temperature range immediately above 80–90 K the rate of methyl groups rotation is near to the free proton frequency, $\omega_H = 9 \times 10^7$ s^{-1} at X-band. Therefore the pseudosecular nuclear transitions terms are expected to give a contribution to the phase memory loss.

The nuclear spin relaxation rate due to this relaxation mechanism is given by (ref. 4)

$$W_n = \frac{1}{60}\left(4\pi^2\ \Delta A_H^2 \frac{\tau_c}{1 + \omega_H^2 \tau_c^2}\right) \tag{9}$$

where τ_c is the correlation time of the methyl reorientation, ω_H is the Larmor frequency of the proton (9×10^7 s^{-1}). The maximum of W_n corresponds to $\tau_c = \omega_H^{-1}$.

From eqn. (8), for $\Delta E/k \approx 1100$ K and $\tau_{\infty C}^{-1} = 10^{12}$ s^{-1}, the condition $\tau_c = \omega_H^{-1}$ will be found at $T \approx 120$ K. Depending on the value of ΔA_H produced by the rotation, the contribution to the phase memory time $1/W_n$ at the latter temperature will range from ≈ 30 μs for $\Delta A_H = 1$ MHz to ≈ 1 μs for $\Delta A_H = 5$ MHz. Therefore we can conclude that in the fast motion régime the pseudosecular relaxation of the methyl protons of tempone could give a contribution in determining

the electron spin phase memory time. A minimum phase memory time for nitroxide radicals in disordered phases was measured by Dzouba and Tsetkov at $T = 120$ K.[28]

From the ENDOR spectrum at $T < 80$ K we know that in this temperature range we have $\tau_C^{-1} < 2\pi\Delta A_H$. In this slow motion régime the contribution to the spin relaxation is due to the lifetime of the hyperfine levels, which is τ_c^{-1}. By calculating the values of τ_c from eqn. (8) with the parameters above, we find that the correlation time of the thermally activated rotational motion of the methyl groups should range from 10 μs at 70 K to 2 s at *ca.* 40 K. Therefore the contribution to the echo dephasing due to the tempone methyl groups rotation can be neglected at low temperature. A contribution to the nuclear spin relaxation from the methyl protons tunneling motion at low temperature has been discussed and modelled by Clough and coworkers.[29,30] However, for hindered methyl protons with an energy barrier as large as the present one, the contribution to the spin relaxation due to the tunneling motion at low temperature can be neglected also.[30]

We now discuss the role of the methyl protons of the host in determining the phase memory time of the guest radical. The protons of the matrix are known to produce dephasing of the electron spins thanks to the random modulation of the local magnetic field due to their nuclear flip–flop transitions.[6] These are due to the flip–flop operators $I_{1\pm}I_{2\mp}$ in the nuclear spin–spin dipolar hamiltonian term. Due to the small value of the nuclear dipolar coupling (42 kHz for the protons of a methylene group), the time modulation of the dipolar interaction induces flip–flop transitions only between nuclei with the same Larmor frequency. The nuclei too near to the paramagnetic center are therefore 'detuned' from the other ones, since they feel the hyperfine field added to the external field.[18]

The random local magnetic field on the paramagnetic centers depends upon the concentration of the protons, see the model by Milov *et al.*[6] This model considers pairs of protons at a distance r_{N-N}, each pair isolated from the other ones. The protons in each pair undergo flip–flop transitions thanks to their dipolar coupling. A simulation of the echo decay at $T = 50$ K for $r_{N-N} = 1.8$ Å gives a gaussian decay that agrees quite well with the experimental decay, see Fig. 5b.

On the other hand, at very low temperature ($T < 20$ K) the echo decays follow an exponential law with square-root time dependent exponent $x = 0.5$, see Table 3.

Two effects not taken into account by the model of Milov *et al.* can become important at low temperature: the collective interactions of the nuclear spins of the matrix, and the tunneling motion of the methyl groups. The possible relevance of the collective interactions between all the nuclei in a matrix, when considering the effect of their flip–flop transition on the electron spin echo, has been pointed out by Salikhov and Tsvetkov.[5] In the crystals of TMCD the model of isolated pairs of interacting protons is particularly unsatisfying, due to the presence of a regular array of very closely spaced methyl groups.

The methyl groups' tunneling is expected to enhance the flip–flop transition probability, as suggested by an obvious extension of the model of proton relaxation due to tunneling methyl groups described in ref. 29. In fact recently it has been observed by Zecevic *et al.*[8] and Lindgren *et al.*,[3] that the rate of electron spin dephasing at low temperature is faster in solvents containing methyl groups. Moreover, the rate of dephasing depends roughly on the barrier hindering the methyl rotation, and solvents with more 'free' methyl groups are more effective in producing the dephasing than the ones with hindered methyl groups.[3,8]

We can compare the T_M phase memory times we have found for the echo decay in the present system with those found in ref. 8 for tempone in glassy mixtures of solvents containing methyl groups at different concentrations. The value of T_M measured in the present work at low temperature fits well with the values obtained in ref. 8 for glassy mixtures of solvents glycerol and *n*-propanol, and 3-methylpentane and decalin, with about the same molar concentration of CH_3 as TMCD (63 M). We do not have any direct information on the energy barrier hindering the rotation of the methyl groups in the TMCD host. However, we can guess that it will be similar to that obtained for tempone, and certainly higher than in the aforementioned solvents used in ref. 8.

Therefore we must conclude that not only the frequency of methyl tunneling, but also other properties of the matrix, as for example its degree of order, must be important in determining the effect of the matrix nuclei on the phase memory time.

It should be noted that also in ref. 8 the value of the exponent x_1 at low temperatures is in some cases smaller than 2 ($0.8 < x_1 < 2$).

A theoretical model for ESE dephasing in presence of tunnelling protons in ordered matrices is still lacking.

ESEEM

Two results obtained in simulating the echo decay modulation are worthy of discussion.

The first one is that the matrix protons do not appear to contribute to the ESEEM at $T > 210$ K. The librational motion above this temperature is expected to be fast enough to average the dipolar coupling of the unpaired electron with the matrix protons.

The second point is the damping of the modulation that has to be introduced to simulate correctly the echo decay, see eqn. (6). In powder systems a damping of the total modulation is expected as a wide distribution of frequencies is present, and interference among them results in a net destroying effect for the total modulation. This is not the case for a single crystal, where modulation frequencies are limited in number. However, recently Nordh and Benetis reported a theoretical study on the modulated echo decay by resolving the Liouville equation for the density matrix, in the presence of chemical exchange at different frequencies k_{ex}.[31] Their results show that for chemical exchange at intermediate rate, *i.e.* when the exchange frequency is similar to the difference between the exchanged resonance frequencies, the nuclear modulation is damped with respect to the fast and slow exchange regions. Therefore we can suppose that the ESEEM damping in our case is due to one of the different exchange processes present for tempone in the crystal.

By comparing the decay times in Tables 3 and 4 one can note that at some temperatures the decay time of the modulation and of the echo are similar, whereas at other temperatures the decay time of the modulation is longer. The interest of this observation comes out if one compares again this behaviour with the theoretical predictions in ref. 31, where it is suggested that the difference between the modulation decay and the echo decay depends on the difference between the relaxation time due to the exchange and the intrinsic T_2 of the exchanging spin packets. In our opinion the comparison of the calculated and experimental results of echo decay in the presence of chemical exchange deserves further work, with experimental results preferably coming from a less dynamically complex system than the present one.

Conclusions

For the first time both the intramolecular and intermolecular dynamics of a spin probe in a solid matrix have been characterized in a wide temperature range. We have shown that different EPR techniques, in particular multifrequency EPR spectroscopy, are necessary in general to fully determine the mechanisms leading to the relaxation behaviour of radicals in solid matrices.

Tempone in a TMCD matrix is performing three types of fast motions for $T > 230$ K, that affect the homogeneous T_2 of the single spin packets, and as expected for 300 K $> T >$ 230 K the echo decay is a linear exponential. The phase memory time becomes so short in the range 130–210 K, due to the effect of conformational interconversion and libration, that no echo can be detected. At $T = 80$ K, the phase memory time reaches its maximum value. This can be explained by assuming that the motions of the probe have slowed down enough at this temperature to minimize the effects of chemical exchange, whereas on the other hand the dephasing effect of the matrix protons are less important than at low temperature.

For $T < 80$ K the effects on spin dephasing due to the interaction with the protons of the matrix become important. We observe a gaussian decay for 50 K $> T >$ 20 K, and a decay depending on the square root of the time for $T < 20$ K. The comparison of the value of the phase memory time at low temperature with a series of values obtained recently on tempone in different matrices[8] confirms the importance of the interaction with methyl protons of the matrix in determining the echo decay.

The time dependence of the echo decay at very low temperature ($T < 20$ K) is not explained by the theoretical models elaborated so far. On the other hand the latter models ignore the effect of tunneling of the methyl protons of the matrix, and of the collective interactions between all the nuclei in it.

From all the results, the role of the rotational motion of the methyl groups in tempone itself in determining the electron spins dephasing at low temperature appear to be negligible.

We can conclude that the ESE decay of nitroxide spin probes at low concentration can be used at very low temperature to obtain information about the nuclear environment of the probe. At higher temperatures intra- and intermolecular dynamics of the radical itself must be taken into account.

Tempone has a twisted-crossover conformation as the minimum energy one. It can be expected that both intra- and intermolecular motions were different for nitroxides with planar or chair conformations, and further work should be done on model systems with probes of the latter type.

The complexity of the mechanisms leading to electron spin relaxation even in this particularly well ordered system is striking, and it should urge, for studies in more complex phases, the exploitation of two-dimensional EPR spectroscopies that provide the extra resolution necessary to disentangle the different relaxation mechanisms.[4]

Acknowledgements

This work has been in part supported by the MURST, and by C.N.R. through its Centro di Studio sugli Stati Molecolari Radicalici ed Eccitati, Padova, and Progetto Strategico Materiali Innovativi. We would like to thank Dr Nikolas Benetis for helpful discussions, Dr E. van Faassen (Utrecht University, The Netherlands) for giving us the possibility of performing ENDOR measurements in his laboratory, and Mrs Sabrina Mattiolo for the preparation of the crystals. One of us, LCB, acknowledges the support from the Human Frontier Science Program (RG-349/94).

References

1 I. Hiromitsu and L. Kevan, *J. Am. Chem. Soc.*, 1987, **109**, 4501; T. Hiff and L. Kevan, *J. Phys. Chem.*, 1989, **93**, 1572; G. Martini, S. Ristori, M. Romanelli and L. Kevan, *J. Phys. Chem.*, 1990, **94**, 7607.
2 M. F. Ottaviani, R. Daddi, M. Brustolon, N. J. Turro and D. A. Tomalia, *Appl. Magn. Reson.*, 1997, **13**, 347; M. F. Ottaviani, P. Matteini, M. Brustolon, N. J. Turro, S. Jockusch and D. A. Tomalia, *J. Phys. Chem. B.*, 1998, **102**, 6029.
3 M. Lindgren, G. R. Eaton, S. S. Eaton, B.-H. Jonsson, P. Hammarström, M. Svensson and U. Carlsson, *J. Chem. Soc., Perkin Trans*, *2*, 1997, 2549.
4 S. Saxena and J. H. Freed, *J. Phys. Chem. A*, 1997, **101**, 7998.
5 K. M. Salikhov and Yu. D. Tsvetkov, in *Time Domain Electron Spin Resonance*, ed. L. Kevan and R. N. Schwartz, Wiley-Interscience, New York, 1979, pp. 231–277.
6 A. D. Milov, K. M. Salikhov, Yu. D. Tsvetkov, *Sov. Phys. Solid State*, 1973, **15**, 802.
7 M. Romanelli, G. Martini, S. Ristori and L. Kevan, *Colloids Surf.*, 1990, **45**, 145.
8 A. Zecevic, G. R. Eaton, S. S. Eaton and M. Lindgren, *Mol. Phys.*, 1998, **95**, 1255.
9 D. E. Budil, K. A. Earle and J. H. Freed, *J. Phys. Chem.*, 1993, **97**, 1294.
10 M. Brustolon, A. L. Maniero and C. Corvaja, *Mol. Phys.*, 1984, **15**, 1269.
11 M. Brustolon, A. L. Maniero and U. Segre, *Mol. Phys.*, 1985, **55**, 713.
12 B. Kirste, A. Krüger and H. Kurreck, *J. Am. Chem. Soc.*, 1982, **104**, 3850.
13 L. Schwartz, A. E. Stillman and J. H. Freed, *J. Chem. Phys.*, 1982, **77**, 5410.
14 I. V. Koptyug, S. H. Bossmann and N. J. Turro, *J. Am. Chem. Soc.*, 1996, **118**, 1345.
15 P. H. Friedlander and J. M. Robertson, *J. Chem. Soc.*, 1956, 3083.
16 F. Mueller, M. A. Hopkins, N. Coron, M. Grynberg, L. C. Brunel and L. C. Martinez, *Rev. Sci. Instrum.*, 1989, **60**, 3681.
17 M. Brustolon, A. Zoleo and A. Lund, *J. Magn. Reson.*, 1999, **137**, 389.
18 A. Abragam, in *The Principles of Nuclear Magnetism*, Oxford University Press, New York, 1983.
19 M. Romanelli and L. Kevan, *Concepts Magn. Reson.*, 1997, **9**, 403; *ibid.*, 1998, **10**, 1.
20 W. B. Mims, *Phys. Rev. B*, 1972, **5**, 2409.
21 M. Iwasaki and K. Toriyama, *J. Chem. Phys.*, 1985, **82**, 5415.
22 M. Brustolon, A. L. Maniero, S. Jovine and U. Segre, *Res. Chem. Intermed.*, 1996, **22**, 359.
23 D. Bordeaux and J. Lajzerowicz, *Acta Crystallogr. B*, 1974, **30**, 790.
24 W. Derbyshire, *Mol. Phys.*, 1962, **5**, 225.
25 J. A. Weil, J. R. Bolton and J. E. Wertz, in *Electron paramagnetic resonance. Theory and practical applications*, Wiley, New York, 1994.
26 S. Clough, A. Heidemann, A. J. Horsewill, J. D. Lewis and M. N. J. Paley, *J. Phys. C: Solid State Phys.*, 1982, **15**, 2495.
27 M. Brustolon, A. L. Maniero, M. Bonora and U. Segre, *Appl. Magn. Reson.*, 1996, **11**, 99.
28 Yu. D. Tsetkov and S. A. Dzuba, *Appl. Magn. Reson.*, 1990, **1**, 179.
29 S. Clough, *J. Phys. C: Solid State Phys.*, 1971, **4**, 2180.
30 J. L. Carolan, S. Clough, N. D. McMillan and B. Mulady, *J. Phys. C: Solid State Phys.*, 1972, **5**, 631.
31 U. E. Nordh and N. P. Benetis, *Chem. Phys. Lett.*, 1995, **244**, 321.

Paper 9/03380G